BBA - Molecular Basis of Disease 1865 (2019) 193–205

Contents lists available at ScienceDirect

BBA - Molecular Basis of Disease

journal homepage: www.elsevier.com/locate/bbadis

Improved cognition, mild anxiety-like behavior and decreased motor performance in pyridoxal phosphatase-deficient mice

Elisabeth Jeanclos[a,*], Monique Albersen[b,1], Rúben J.J. Ramos[b], Annette Raab[a,c], Christian Wilhelm[a], Leif Hommers[a,c,d], Klaus-Peter Lesch[c,d,e,f,g], Nanda M. Verhoeven-Duif[b], Antje Gohla[a,*]

[a] Institute of Pharmacology and Toxicology, University of Würzburg, Germany
[b] Department of Genetics, University Medical Center Utrecht, the Netherlands
[c] Interdisciplinary Center for Clinical Research, University Hospital Würzburg, Germany
[d] Comprehensive Heart Failure Center, University Hospital Würzburg, Germany
[e] Division of Molecular Psychiatry, Center of Mental Health, University of Würzburg, Germany
[f] Laboratory of Psychiatric Neurobiology, Institute of Molecular Medicine, I.M. Sechenov First Moscow State Medical University, Moscow, Russia
[g] Department of Neuroscience, School for Mental Health and Neuroscience, Maastricht University, Maastricht, the Netherlands

ARTICLE INFO

Keywords:
Pyridoxal phosphatase
Vitamin B6
γ-Aminobutyric acid (GABA)
Motor performance
Neuropsychiatric diseases
Neurotransmitter biosynthesis

ABSTRACT

Pyridoxal 5′-phosphate (PLP) is an essential cofactor in the catalysis of ~140 different enzymatic reactions. A pharmacological elevation of cellular PLP concentrations is of interest in neuropsychiatric diseases, but whole-body consequences of higher intracellular PLP levels are unknown. To address this question, we have generated mice allowing a conditional ablation of the PLP phosphatase PDXP. Ubiquitous PDXP deletion increased PLP levels in brain, skeletal muscle and red blood cells up to 3-fold compared to control mice, demonstrating that PDXP acts as a major regulator of cellular PLP concentrations *in vivo*. Neurotransmitter analysis revealed that the concentrations of dopamine, serotonin, epinephrine and glutamate were unchanged in the brains of PDXP knockout mice. However, the levels of γ-aminobutyric acid (GABA) increased by ~20%, demonstrating that elevated PLP levels can drive additional GABA production. Behavioral phenotyping of PDXP knockout mice revealed improved spatial learning and memory, and a mild anxiety-like behavior. Consistent with elevated GABA levels in the brain, PDXP loss in neural cells decreased performance in motor tests, whereas PDXP-deficiency in skeletal muscle increased grip strength. Our findings suggest that PDXP is involved in the fine-tuning of GABA biosynthesis. Pharmacological inhibition of PDXP might correct the excitatory/inhibitory imbalance in some neuropsychiatric diseases.

1. Introduction

Pyridoxal 5′-phosphate (PLP), the co-enzymatically active form of vitamin B6, is one of the most versatile cofactors found in nature. In mammals, PLP-dependent enzymes catalyze ~140 different types of biochemical transformations, including reactions that are required for neurotransmitter-, amino acid- and glycogen metabolism [1]. PLP is a highly reactive aldehyde that transiently forms a Schiff base with the ε-amino group of the active site lysine in its cognate apo-enzymes [2]. It is thought that intracellular PLP concentrations and PLP trafficking are tightly controlled to ensure sufficient PLP supply to apo-enzymes, while minimizing free PLP levels. This is important to prevent non-specific reactions of PLP with cellular nucleophiles and proteins that are not B6 enzymes [3–5].

Intracellular PLP levels depend on the availability and -transport of PLP precursors [6], the biosynthetic activities of pyridoxal 5′-kinase (PDXK) and pyridox(am)ine 5′-phosphate oxidase (PNPO), the extent of PLP scavenging by proteins and small molecules, PLP binding to carriers such as PROSC, PDXK and PNPO, and PLP hydrolysis by pyridoxal 5′-phosphate phosphatase (PDXP) [3,4,7]. Specifically, PDXK catalyzes the phosphorylation of pyridoxine (PN), pyridoxamine (PM) or pyridoxal (PL) to their 5′-phosphorylated variants PNP, PMP or PLP. PNPO additionally (re)generates PLP from PNP or PMP by catalyzing the oxidation of their respective hydroxyl or amino groups to the co-enzymatically essential

* Corresponding authors.
E-mail addresses: elisabeth.jeanclos@uni-wuerzburg.de (E. Jeanclos), antje.gohla@uni-wuerzburg.de (A. Gohla).
[1] Current address: Department of Clinical Chemistry, VU Medical Center, Amsterdam, the Netherlands.

https://doi.org/10.1016/j.bbadis.2018.08.018
Received 29 June 2018; Received in revised form 13 August 2018; Accepted 14 August 2018
Available online 16 August 2018

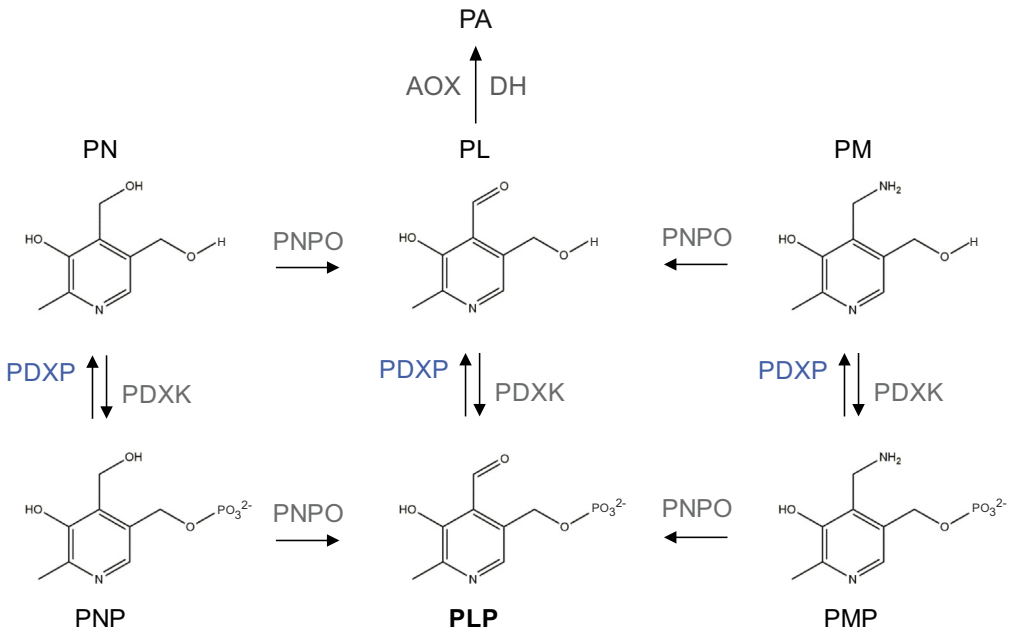

Fig. 1. Enzymes involved in mammalian PLP metabolism. PA, 4′-pyridoxic acid; PN(P), pyridoxine (-5′-phosphate); PL(P), pyridoxal (-5′-phosphate); PM(P), pyridoxamine (-5′-phosphate). PDXP, pyridoxal phosphatase; PDXK, pyridoxal kinase; PNPO, pyridox(am)ine oxidase; AOX/DH, aldehyde oxidase/β-NAD dehydrogenase. PL is oxidized to PA in the liver and excreted into the urine. Catalytic efficiencies (k_{cat}/K_M) of PDXP: PLP, $6.1 \times 10^5\,M^{-1} \times s^{-1}$; PNP, $2.7 \times 10^4\,M^{-1} \times s^{-1}$; PMP, $5.6 \times 10^3\,M^{-1} \times s^{-1}$ [8].

aldehyde moiety of PLP [3] (Fig. 1). The pathways of PLP biosynthesis have been established for decades, yet a dedicated PLP phosphatase (PDXP) was cloned more recently [8]. PDXP activity may play a significant role in the regulation of cellular PLP concentrations [7,8]. Nonetheless, the relative importance of PDXP for the regulation of PLP homeostasis and for PLP-dependent functions *in vivo* is unknown.

A pharmacological elevation of cellular PLP concentrations is of interest in neuropsychiatric disorders and inflammation [9–11]. Inborn errors of vitamin B6 metabolism can lead to inadequate levels of PLP in the brain and cause childhood epilepsy [4,12–17]. In these cases, the administration of PLP or PN leads to prompt seizure cessation. However, high doses of PN can cause respiratory depression, and impose treatment withdrawal [4]. Individuals with B6-dependent epilepsy often require continuous oral PN supplementation, yet long-term treatment with high doses of PN or PLP can be toxic [18–20]. A pharmacological inhibition of PDXP [21] might circumvent toxic effects caused by elevated extracellular B6 vitamer levels, and provide a novel approach to increase cellular PLP concentrations.

The aim of the present study was to analyze the relative importance of PDXP for the regulation of tissue PLP concentrations, and to explore the biochemical and behavioral consequences of PDXP deletion in gene-targeted mice. Our results demonstrate that PDXP is a major factor in the control of cellular PLP concentrations *in vivo*, and we uncover a previously unexploited approach to increase GABA levels in the brain. PDXP loss improved spatial learning and memory, but also caused a mild anxiety-like phenotype and central nervous system-dependent muscle weakness. Further research is necessary to evaluate whether pharmacological PDXP inhibition might be an advantageous strategy to increase cellular PLP levels.

2. Materials and methods

2.1. Materials

Unless otherwise specified, all reagents were of the highest available purity and purchased from Sigma-Aldrich.

2.2. Generation and breeding of Pdxp knockout mice

Floxed *Pdxp* mice (*Pdxp*^{tm1Goh}) were generated on a C57Bl/6J background by Ozgene Pty Ltd., Australia. The neomycin resistance cassette was removed by breeding with the global FLPe deleter strain B6.129S4-Gt(ROSA)26Sor < tm1(FLP1)Dym > /RainJ. Whole-body, skeletal muscle or neural cell-directed *Pdxp* knockouts were achieved by breeding with B6.FVB-Tg(EIIa-cre)C5379Lmgd/J (EIIa-Cre), B6.Cg-Tg(ACTA1-cre)79Jme/J (Acta1-Cre), or B6.Cg-Tg(Nes-cre)1Kln/J (Nestin-Cre) transgenic mice obtained from The Jackson Laboratory. Mouse experiments were approved by the local authorities (Regierung Unterfranken), and all analyses were carried out in strict accordance with all German and European Union applicable laws and regulations concerning care and use of laboratory animals.

2.3. Genotyping

Genomic DNA was isolated with DNeasy (Qiagen) and digested with EcoRV. Southern blotting was performed according to standard procedures. Briefly, DNA was subjected to agarose gel electrophoresis, denatured, blotted onto nitrocellulose and crosslinked with UV light. The probe was generated by PCR using Pfx polymerase (Invitrogen) and labeled with [α-^{32}P] dCTP (Hartmann Analytic), employing the DecaPrime II DNA labeling kit (Ambion). Unincorporated labeled nucleotides were removed with Illustra ProbeQuant G-50 micro columns (GE Healthcare). Genotyping of Acta1-Cre and Nestin-Cre transgenic mice was performed by PCR as described by The Jackson Laboratory.

2.4. Tissue sample preparation

Mice were sacrificed by cervical dislocation and perfused with PBS. Skeletal muscle samples were taken from the upper back hind limb, and contained *musculus biceps femoris*, *musculus semimembranosus* and *musculus semitendinosus*. Small intestine samples (comprising duodenum, jejunum and ileum) were cut into small segments and washed extensively with phosphate-buffered saline (PBS). For liver analysis, the entire organ was used. Brains were either used *in toto*, or different brain regions were dissected. To this end, the brain was placed on an ice-cold adult mouse brain slicer (Harvard Apparatus). A 3 mm coronal section was cut starting from the basis of the circle of Willis towards the frontal part of the brain (Bregma −3.16 to Bregma 0.02), and the brain cortex and the midbrain region (containing hippocampus, hypothalamus and thalamus) were dissected from this slice. All brain parts including cerebellum and hindbrain were weighed (wet weight). Pups were sacrificed by decapitation on postnatal day 6 (P6), and brains were

dissected, weighed and flash-frozen in liquid nitrogen. For analysis, organs and tissue parts were homogenized in ice-cold PBS with a Potter S homogenizer (Sartorius). Proteins were precipitated with 10% (w/v) 6.1-N trichloroacetic acid (TCA) for 15 min on ice with occasional vortexing. After centrifugation (20,000 ×*g*, 15 min, 4 °C), supernatants were flash-frozen in liquid nitrogen and kept at −80 °C.

2.5. Plasma and red blood cell preparation

Heparinized blood was centrifuged at room temperature (800 ×*g*, 10 min). The supernatant (plasma) was centrifuged again, and proteins in the supernatant were removed by precipitation, using 10% (w/v) 6.1-N TCA. Packed red blood cells (RBCs) were washed by centrifugation and resuspension in 0.9% (w/v) NaCl. Cells were lysed and proteins were precipitated by adding 10% 6.1-N TCA. Plasma and RBC extracts were flash-frozen in liquid nitrogen and kept at −80 °C until analysis. To calculate the intracellular concentrations of B_6 vitamers, the intracellular RBC volume was estimated to correspond to 52% of the packed RBC volume.

2.6. Quantification of B_6 vitamers, GABA and amino acids

B_6 vitamers, GABA and other amino acids were quantified using UPLC-MS/MS as described [6,22–24].

2.7. Neurotransmitter analysis by HPLC

Mice were sacrificed by cervical dislocation, brains were dissected, weighed and flash-frozen in liquid nitrogen. The entire procedure was performed in < 3 min. Frozen brains were sonicated (2 × 30 s) in a 0.3 M perchloric acid solution at 4 °C, and samples were centrifuged (16,000 ×*g*, 10 min, 4 °C). Supernatants were analyzed on a Dionex Ultimate 3000 HPLC (ThermoScientific), using 75 mM NaH_2PO_4, 1.5 mM octane sulfonic acid, 10% (v/v) acetonitrile; pH 3 as a mobile phase. Neurotransmitters were separated on a 3 µm reverse phase column (BDS-HYPERSIL-C18, ThermoScientific) and detected by electrochemical reaction at 450 mV.

2.8. Western blot analysis

Tissue or cell homogenates were prepared as detailed above and extracted with RIPA buffer [50 mM Tris, pH 7.5; 150 mM NaCl, 1% (v/v) Triton X-100, 0.5% (v/v) sodium deoxycholate, 0.1% (w/v) SDS, 1 mM 4-(2-aminoethyl)benzenesulfonyl fluoride (Pefabloc), 5 µg/mL aprotinin, 1 µg/mL leupeptin, 1 µg/mL pepstatin] for 15 min at 4 °C under rotation, and lysates were clarified by centrifugation (20,000 ×*g*, 15 min, 4 °C). Protein concentrations in the supernatants were determined using the Micro BCA Protein Assay Kit (Thermo Scientific). Samples were solubilized in Laemmli buffer and subjected to standard immunoblotting. The following antibodies were used: Cell Signaling Technology, α-PDXP (clone C85E3) and α-GAPDH (clone 14C10); Merck/Millipore, α-actin (mAb1501) and α-FAK (clone 4.47); ThermoFisher Scientific, α-PNPO (#PA5-26400); and Sigma Aldrich, α-PDXK (AB1, #AV53615). To analyze Ser3-phosphocofilin and cofilin levels, tissues were dissected from 4-months old male mice, and immediately flash-frozen in liquid nitrogen as described above. Frozen tissues were then pulverized using a pre-cooled porcelain mortar and pestle. About 50–100 mg of this powder was solubilized in 250 µL ice-cold lysis buffer [20 mM Tris, pH 7.5; 150 mM NaCl, 1% (v/v) Triton X-100, 1 mM β-glycerophosphate, 2.5 mM sodium pyrophosphate, 1 mM sodium orthovanadate, 1 mM Pefabloc, 1 µg/mL leupeptin/aprotinin/pepstatin; 1/1000 phosphatase inhibitor cocktail I and II (both from Sigma Aldrich, #P2850 and P5726)] for 2 h at 4 °C under rotation. Lysates were cleared by centrifugation (20,000 ×*g*, 15 min, 4 °C), and protein concentrations in the supernatants were determined and adjusted to ~20 µg/µL using the Micro BCA Protein Assay Kit. Samples were diluted to a final concentration of ~2 µg/µL in 2× Laemmli buffer, and ~40–50 µg of proteins were separated on a 12% SDS-PAGE gel. For hippocampal extracts, ~200 µg of proteins were analyzed. Proteins were semi-dry transferred to nitrocellulose and immunoblotted using α-Ser3-phosphocofilin antibodies (clone 77G2, Cell Signaling Technology). Blots were stripped and reprobed using α-cofilin antibodies (#3312, Cell Signaling Technology or #ACFL02, Cytoskeleton Inc.).

2.9. Behavioral studies

2.9.1. Animals

All animals were housed at the Center for Experimental Molecular Medicine at the University of Würzburg, and were kept on a regular 14/10 h light-dark cycle, in a temperature (21 ± 0.5 °C)- and humidity (50 ± 5%)-controlled environment with *ad libitum* access to food and water. All experiments were performed by the same experienced female investigator between 9 a.m. and 3 p.m. All mice were males housed in groups of 2–5 animals per cage. The age of the mice is specified in the respective figures. All animal protocols were in line with the provisions of the Animal Protection Law according to the Directive of the European Communities Council of 1986 (86/609/EEC). Unless otherwise indicated, behavioral tests were performed according to standard procedures using devices from TSE Systems. Mice were imaged with an infrared light-sensitive CCD camera, and data were collected and analyzed using the automated tracking software VideoMot2 (TSE Systems).

2.9.2. Tests for anxiety-like behavior, exploratory behavior, and spatial learning and memory

Mouse behavior in the open field arena, the elevated plus maze, the dark-light box and in the Barnes maze was evaluated as described [25]. An independent cohort of mice was analyzed in the Barnes maze; bright light (~100 lx) was used as a mildly aversive stimulus. Marble burying was performed as published [26]. Briefly, a standard mouse cage (42.5 × 26.5 × 15 cm) was filled with ~5 cm bedding material. Eighteen glass marbles were spaced evenly in a 3 × 6 grid-fashion on the surface of the bedding. Mice were placed in the cage for 30 min, and the number of marbles buried up to 2/3 of their depth was counted.

2.9.3. Sucrose preference test

In a two-bottle free choice test measuring the preferred intake of either sucrose solution or regular water, mice typically prefer sweetened water. A reduction in the sucrose preference ratio in mice is considered to be indicative of anhedonia, a core symptom of depression in humans [27]. Mice were presented with two drinking bottles in their home cage, one containing plain tap water and the other filled with a 2% (w/v) sucrose solution as described elsewhere [27]. The beginning of the test started with the onset of the dark (active) phase of the animals' cycle. No food or water deprivation was applied prior to the test. The position of the two bottles was switched daily to reduce any possible confounding effect due to a side-bias, and mice were tested for a total of nine days. The consumption of water and sucrose solution was estimated simultaneously in control and experimental groups by weighing the bottles. The sucrose preference ratio was calculated as the percentage of sucrose intake relative to the total volume of fluid intake using the following equation: Volume (sucrose solution) / [volume (sucrose solution) + volume (water)] × 100 [28].

2.9.4. Inverted screen test

Each mouse was placed on a standard cage lid and allowed to obtain a firm grip. The lid was then swiftly inverted over an empty mouse cage filled with bedding. The time until the mouse fell into the empty cage was measured using a stopwatch; maximum test duration was 5 min. Mice were given three trials each day with a 20 s recovery phase in between trials. The test was repeated on three consecutive days. The cage lid was cleaned before testing another mouse. Latency to fall into the cage was used to evaluate limb strength.

2.9.5. Weights test

The weights test was performed as described [29], with the exception that mice were allowed to hold the wire mesh with all four limbs. Briefly, mice were held by the middle of their tails and allowed to grasp a fine wire mesh with an increasing number of steel chain links attached to it. The mice grasping the wire mesh with the attached weights were lifted, and the time they held on to the weight was measured with a stopwatch. The criterion was a 3 s hold; if the mouse dropped the weight earlier, the test was repeated twice after a recovery phase of 10 s. Failure to hold a given weight three times terminated the trial. If the mouse succeeded in holding the weight, the next heaviest weight was tested. The test score indicates the number of links in the heaviest chain that the mouse held for 3 s multiplied by the time (in s) it held on to it. For example, a score of 15 indicates a mouse holding a 5-link weight for 3 s; a score of 16 indicates that it held a 5-link weight for 3 s and a 6-link weight for 1 s. The weight of each chain was 13 g, the weight of the mesh attached to the chains links was 5 g.

2.9.6. Grip strength

Hind paw strength was determined using an automated Grip Strength Meter (Columbus Instruments) as reported previously [30]. In short, mice were trained to grasp a bar with either their front or hind paws. A pull was exerted, and the maximal strength that the mice exhibited before releasing the grip bar was measured. For each mouse, ten measurements per day were acquired on three consecutive days. The average grip strength value (in N) was determined for each mouse, and values were expressed relative to the mean values of the respective control cohort.

2.10. Image quantification and statistical analysis

Western blots were quantified with NIH ImageJ, version 1.45i. For statistical analysis, two-tailed, unpaired Student's *t*-tests were performed using GraphPad Prism version 6.0. All samples that were subjected to statistical analysis were biological replicates. The number of independent samples or individual mice per group and genotype is specified in each figure or figure legend. Reprobes of Western blot experiments were performed using the same membrane that was probed for the primary protein under study.

3. Results

3.1. PDXP is a dominant regulator of pyridoxal 5′-phosphate levels in vivo

To study the functions of PDXP *in vivo*, we generated conditionally *Pdxp*-deficient mice (Supplementary Fig. S1A). Southern blot analysis demonstrated homologous recombination after breeding $Pdxp^{flx/flx}$ mice with the whole-body Cre deleter strain EIIa-Cre (Supplementary Fig. S1B). Homozygous *Pdxp*-deficient (KO) mice on a C57BL/6J background were born at the expected Mendelian frequencies, and were indistinguishable from wildtype (WT) controls in terms of viability, growth and fertility. Fig. 2A demonstrates efficient PDXP deletion in all investigated organs and cells at the protein level. In accordance with the important role of the PDXP substrate pyridoxal 5′-phosphate (PLP) for neurotransmitter biosynthesis and metabolism, PDXP was highly expressed in the brain. The identity of the ~25 kDa band that specifically reacts with the α-PDXP antibody in WT, but not in PDXP-KO

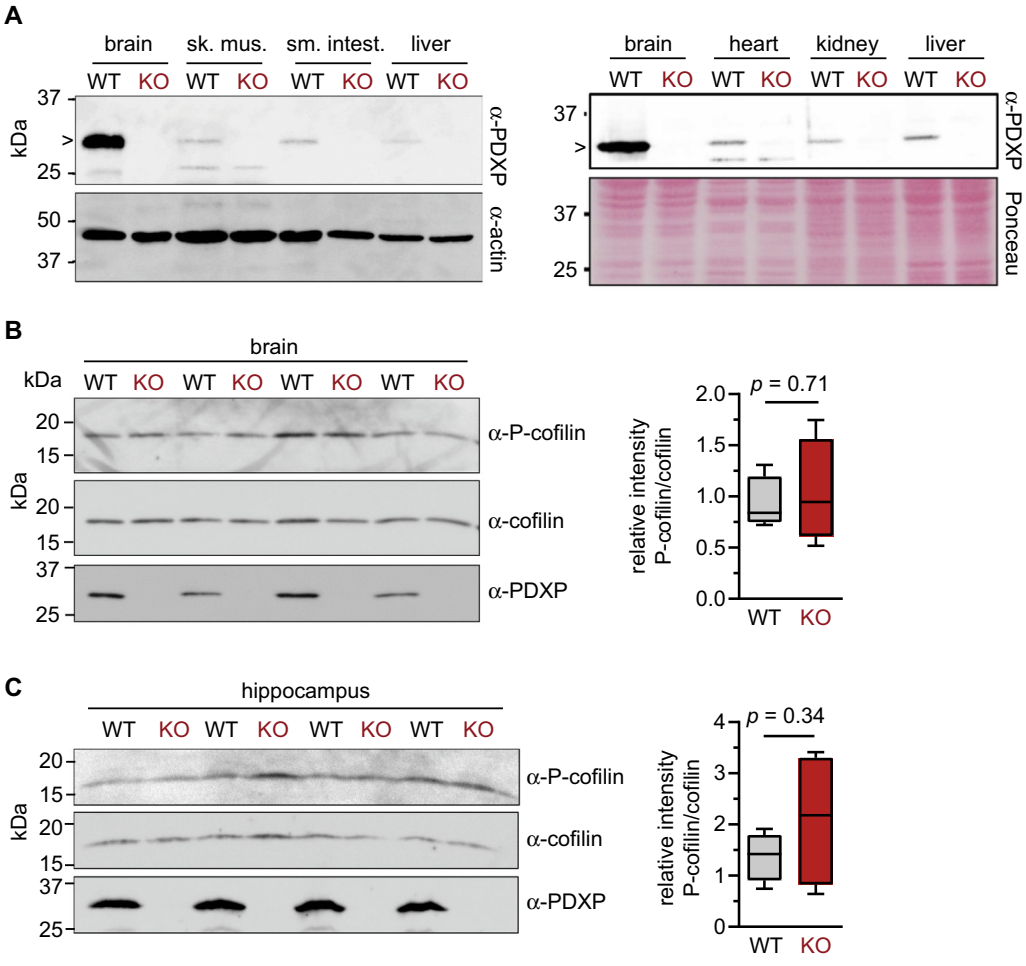

Fig. 2. Characterization of conditionally PDXP-deficient mice. (A) Western blot analysis of PDXP expression in different wildtype (WT) mouse organs, and loss of detectable PDXP expression in $Pdxp^{flx/flx}$; *EIIa-Cre* mice (KO). Data are representative of $n \geq 3$ assays performed with tissues dissected from at least three different WT and three different KO mice. The position of the ~32 kDa PDXP protein is indicated by an arrowhead. The identity of the ~25 kDa band is currently unknown. (B, C) Effect of PDXP deletion on Ser3-phosphocofilin (P-cofilin) levels in whole brain (B) or hippocampal lysates (C); $n = 4$ mice per genotype were analyzed. P-cofilin signals were normalized to the respective cofilin signals; the densitometric quantification is shown on the right. The whiskers indicate minimum and maximum values. Samples in (A) were obtained from 7 to 8 months-old male mice; samples in (B) and (C) were from 4 months-old male mice. Whole-brain lysates in (B) and hippocampal lysates (C) were generated from two separate mouse cohorts. Sk. mus., skeletal muscle; sm. intest., small intestine.

brains is currently unclear. Because PDXP isoforms of a corresponding molecular mass are not known to exist, this band might represent a proteolytic PDXP degradation product.

After the molecular cloning of PDXP [8], an enzyme termed chronophin was isolated from bovine brain fractions and shown to dephosphorylate the actin regulatory protein cofilin on serine-3 [31]; surprisingly, chronophin and PDXP turned out to be identical. PDXP/chronophin can regulate cofilin-dependent actin re-organization at the leading edge of immune and cancer cells [32–35], and mediate an ATP-sensing mechanism for cofilin dephosphorylation in neuronal cells exposed to energy-stress [36]. In addition, it has recently been reported that the constitutive genetic ablation of *Pdxp* (referred to in that work as PLPP/CIN) leads to a moderate, ~45% increase in cofilin phosphorylation in the mouse hippocampus; conversely, substantial transgenic overexpression of the phosphatase resulted in a ~30% decrease in cofilin phosphorylation levels [37]. We analyzed the phosphocofilin/cofilin ratio in lysates of whole brain (Fig. 2B) and isolated hippocampi (Fig. 2C) in our mouse model. Phosphocofilin levels were more variable in PDXP-KO than in WT samples, but we did not detect significant PDXP-dependent changes.

UPLC-MS/MS-based quantification of PLP, the primary known *in vitro* metabolite substrate of PDXP [7,8,38], revealed threefold increases in PLP levels in whole brain extracts of adult PDXP-KO compared to WT mice. PLP levels were also significantly elevated in skeletal muscle and in red blood cells. We did not find PLP changes in liver, in the small intestine or in plasma (Fig. 3A, Table 1). These findings indicate that PDXP is not involved in the regulation of extracellular PLP levels, and suggest that PDXP is not essential for PLP hydrolysis in liver and intestine. However, in contrast to the brain, liver can release PLP into the plasma, and secreted PLP can subsequently be hydrolyzed to PL by alkaline phosphatase, a membrane-bound ectoenzyme. It is therefore possible that PDXP loss in the liver impacts intracellular PLP levels, but that this effect is undetectable due to PLP secretion and extracellular PLP hydrolysis [39]. Likewise, the loss of PDXP in the small intestine [6] might be compensated for by direct PLP transfer from the intestinal lumen to the circulation, or by alkaline phosphatase activity [40]. The lack of increased PLP levels in the plasma of PDXP-KO mice is consistent with a critical role of the extracellular, tissue non-specific alkaline phosphatase TNAP for PLP hydrolysis in plasma, as revealed by the markedly elevated plasma PLP levels measured in patients with hypophosphatasia, an inborn error characterized by impaired TNAP activity [41], and by the increased plasma PLP concentrations found in TNAP-targeted mice (ref. [42] and see below).

Further analysis of the adult brain demonstrated that PDXP loss led to a comparable PLP increase in all investigated areas (cortex, midbrain, hindbrain and cerebellum). We also observed a ~twofold increase in PLP levels in the brains of 6 day-old (postnatal day 6, P6) PDXP-KO pups (Fig. 3B, Table 2). In brain, PL levels also increased in a PDXP-dependent manner (Tables 1, 2). However, because the relative increases in PL and PLP levels were similar in PDXP-KO brain extracts, we speculate that extracellular TNAP partially hydrolyzed PLP to PL during cell lysis [42,43]. PN levels in whole-brain extracts of adult PDXP-KO mice appeared to be increased (Table 1), but the analysis of different adult brain regions or of P6 brains did not confirm this result (Table 2). By comparison, mice lacking TNAP have reduced PLP levels in the brain, but strongly elevated PLP levels in plasma (brain: WT, 4.5 ± 1.0 nmol/g wet tissue weight; TNAP-KO, 1.6 ± 0.3 nmol/g wet tissue weight; serum: WT, 183 ± 104 nM; TNAP-KO, 3166 ± 1288 nM, ref. [42]). Taken together, these data clearly demonstrate that PDXP is a key determinant in the control of cellular PLP concentrations *in vivo*.

A presumed primary function of PDXP is to keep the levels of free intracellular PLP low. This is important for cellular homeostasis because PLP is an electrophilic small molecule that can bind and inactivate cellular nucleophiles. In addition, elevated PLP levels may impinge upon cellular PLP biosynthesis. *In vitro*, PLP functions as an effective product inhibitor of PNPO, and it additionally binds PNPO tightly at a non-catalytic site [35,36]. We therefore investigated whether elevated levels of PLP influenced PNPO. Western blot analysis of PNPO expression revealed ~2.4-fold higher PNPO levels in PDXP-KO compared to WT brain lysates. In contrast, PDXK expression was not significantly altered (Fig. 3C). It is possible that higher intracellular PLP levels enhance PNPO stability and half-life. Alternatively, elevated PLP levels might inhibit PNPO activity, and trigger a compensatory increase in PNPO protein expression.

3.2. Effect of PDXP loss on amino acid levels in the brain

Because PLP is an essential cofactor of many enzymes involved in amino acid metabolism [1], we next asked whether elevated PLP levels affected steady-state amino acid levels in the adult brain. As shown in the Supplementary Table S1, changes were restricted to a subset of amino acids in particular brain regions. Serine and alanine levels were significantly increased in the cortex (+14% or +21%, respectively), and citrulline levels were higher in the basal ganglia region (+14%). Glutamine and glycine concentrations decreased in PDXP-KO hindbrains (−20% or −13%, respectively). The levels of pipecolic acid, a catabolite of lysine, were higher in all parts of the brain, with increases ranging from +23% in the midbrain to +33% in the cortex. In developing PDXP-deficient brains at P6, alanine and threonine levels were elevated (+13% or +35%, respectively), and methionine and phenylalanine levels were reduced (−35% or −43%, respectively). Together, these data indicate that higher intracellular PLP concentrations affect amino acid metabolism, but do not lead to a general increase in the activities of PLP-dependent enzymes.

3.3. Elevated GABA levels and improved spatial learning and memory in PDXP-KO mice

PLP is an obligatory cofactor for decarboxylation reactions in the biosynthesis of dopamine, (nor)epinephrine, serotonin and GABA. Specifically, PLP is required for the aromatic L-amino acid decarboxylase, which catalyzes the decarboxylation of L-3,4-dihydroxyphenylalanine (DOPA) to the (nor)epinephrine precursor dopamine, and the decarboxylation of 5-hydroxy-L-tryptophan to 5-hydroxytryptamine (serotonin) [44]. Quantification of these neurotransmitters and their catabolites in brain extracts of 9 months-old male mice did not show PDXP-dependent changes (Fig. 4A). Thus, elevated cellular PLP concentrations did not increase the physiological activity of DOPA decarboxylase. Interestingly though, we found significantly higher amounts of GABA in whole brain extracts of 8 months-old PDXP-KO mice, as well as in the cerebellar and midbrain region of 4 months-old PDXP-KO mice (Fig. 4B). GABA concentrations were also significantly higher in whole brains and in dissected cerebellae of P6 PDXP-KO compared to WT pups (Fig. 4B). The rate-limiting step in GABA biosynthesis consists of the PLP-dependent decarboxylation of glutamate [45,46]; glutamate itself is formed by glutamate transaminase, which also uses PLP as a cofactor. Yet, similar to dopamine, epinephrine and serotonin, the amounts of glutamate were comparable between 4 months-old PDXP-KO and WT mice (Fig. 4C). We conclude that loss of PDXP expression results in a selective increase in cerebral GABA levels.

One distinguishing feature of GABA biosynthesis is that it is mediated by two glutamate decarboxylases, which are encoded by separate genes [47]. The majority of GABA in the brain is synthesized by the 67 kDa glutamate decarboxylase (GAD67), a constitutively active, cytosolic enzyme that is typically saturated with PLP. In contrast, the 65 kDa glutamate decarboxylase (GAD65) is enriched in synapses and bound to the membranes of synaptic vesicles. GAD65 predominantly exists as an inactive apo-enzyme in cells, and PLP-binding transiently increases holo-GAD65 formation in response to the demand for extra GABA in neurotransmission [46,48,49]. Although overall GABA

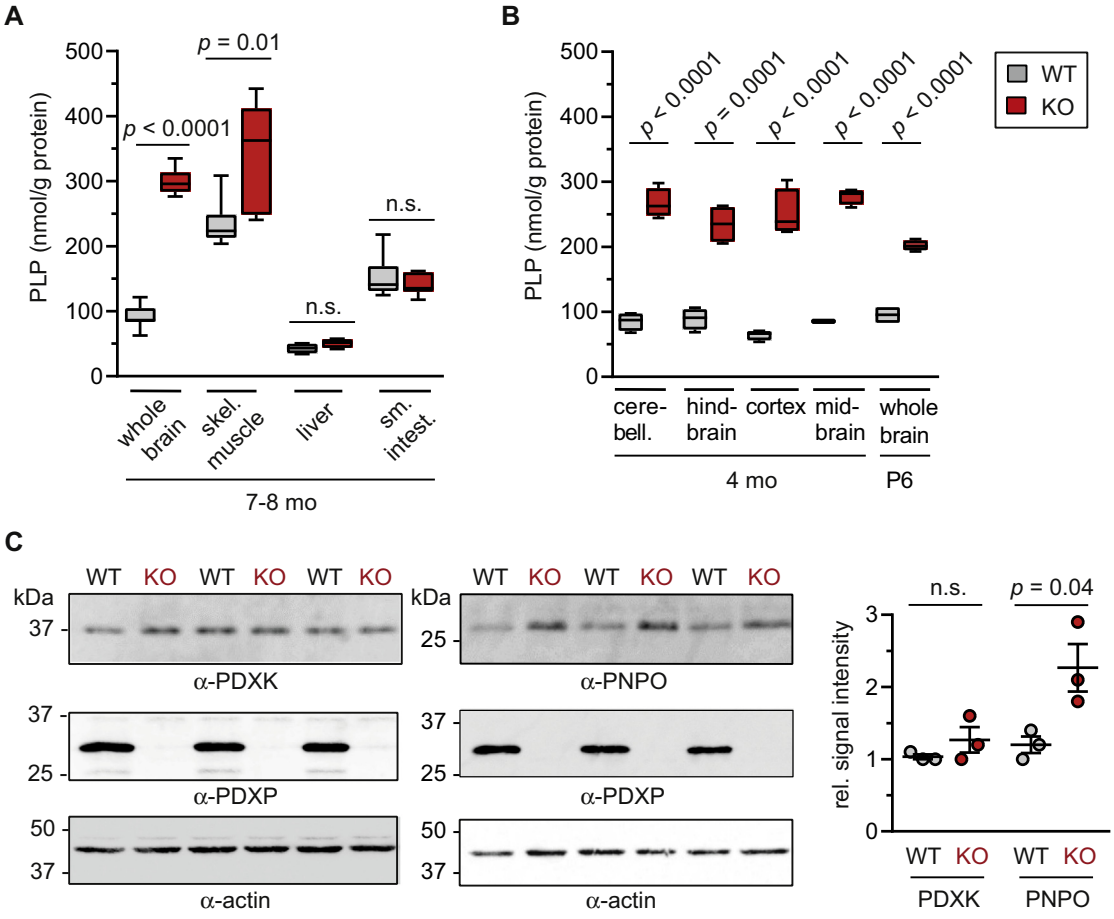

Fig. 3. Effect of whole-body PDXP deletion on PLP levels *in vivo*. PLP levels were quantified by UPLC-MS/MS. (A) Organs were isolated from 7 to 8 months-old male mice, n = 4–8 per genotype; the indicated brain regions were dissected from 4 months-old male mice, n = 4 per genotype (B). The whiskers indicate minimum and maximum values. For further details and data on other B6 vitamers, see Tables 1 and 2. (C) Western blot analysis of PDXK and PNPO levels in whole brain lysates of 7–8 months-old male mice; lysates of n = 3 mice per genotype were analyzed. Right panel, blots were analyzed densitometrically after normalization to actin. WT, wildtype mice; KO, *Pdxp*$^{flx/flx}$; *EIIa-Cre* mice. Data in (C) are mean values ± S.E.M.; n.s., non-significant. Skel. muscle, skeletal muscle; sm. intestine, small intestine; cerebell., cerebellum; P6, postnatal day 6.

Table 1
UPLC-MS/MS-based quantification of B_6 vitamers in WT and PDXP-KO mice.

	nmol/g protein	*n*	PLP	PL	PA	PMP	PM	PN
Brain	WT	8	91.29 ± 6.30	25.54 ± 1.56	0.27 ± 0.09	156.1 ± 13.6	0.79 ± 0.20	0.06 ± 0.01
	PDXP-KO	7	298.8 ± 7.45	74.95 ± 5.95	0.35 ± 0.12	173.6 ± 10.2	1.3 ± 0.24	0.33 ± 0.05
	p-Value		< 0.0001	< 0.0001	0.60	0.33	0.12	< 0.0001
Skeletal muscle	WT	8	235.0 ± 12.0	5.10 ± 1.62	0.05 ± 0.02	75.65 ± 13.17	0.66 ± 0.26	0.01 ± 0.01
	PDXP-KO	7	331.4 ± 31.9	8.83 ± 3.40	0.13 ± 0.05	98.69 ± 28.22	0.79 ± 0.35	0.02 ± 0.02
	p-Value		0.01	0.32	0.12	0.45	0.77	0.74
Small intestine	WT	4	42.75 ± 3.77	7.80 ± 0.66	0.42 ± 0.23	97.25 ± 15.73	0.46 ± 0.12	0.01 ± 0.01
	PDXP-KO	4	50.77 ± 3.56	6.62 ± 0.05	0.69 ± 0.12	116.3 ± 3.6	0.71 ± 0.08	0.41 ± 0.17
	p-Value		0.17	0.12	0.34	0.28	0.14	0.06
Liver	WT	8	152.5 ± 10.9	4.32 ± 0.84	0.68 ± 0.13	222.9 ± 14.3	0.28 ± 0.09	0.024 ± 0.01
	PDXP-KO	7	140.9 ± 6.2	3.86 ± 0.56	0.60 ± 0.13	223.7 ± 9.6	0.24 ± 0.06	0.017 ± 0.01
	p-Value		0.39	0.66	0.64	0.96	0.70	0.60

	nmol/L	*n*	PLP	PL	PA	PMP	PM	PN
Plasma	WT	8	146.9 ± 14.9	528.0 ± 45.2	85.88 ± 12.92	246.9 ± 41.2	n.d.	n.d.
	PDXP-KO	7	143.4 ± 9.3	483.7 ± 33.3	65.14 ± 6.86	142.4 ± 23.2	n.d.	n.d.
	p-Value		0.85	0.45	0.2	0.05		
Red blood cells	WT	8	3776 ± 468	393.4 ± 31.4	14.91 ± 1.81	347.4 ± 23.5	n.d.	n.d.
	PDXP-KO	7	10,321 ± 1402	332.9 ± 23.0	10.20 ± 2.55	389.5 ± 53.2	n.d.	n.d.
	p-Value		< 0.001	0.15	0.15	0.46	–	–

Shown are mean values ± S.E.M. *N* indicates the number of analyzed mice. For comparison with the other B_6 vitamers, results of the PLP measurements depicted in Fig. 3A and B are shown again here. Pyridoxine 5′-phosphate (PNP) could not be detected. Statistically significant differences between the two genotypes were analyzed using unpaired *t*-tests. All mice were 7–8 months-old males; n.d., not determined.

Table 2
UPLC-MS/MS-based quantification of B_6 vitamers in the brains of adult and postnatal WT and PDXP-KO mice.

	nmol/g protein	*n*	PLP	PL	PA	PMP	PM	PN
Cerebellum	WT	4	85.10 ± 7.05	9.18 ± 0.69	0.032 ± 0.03	162.1 ± 22.46	0.14 ± 0.02	0.01 ± 0.01
	PDXP-KO	4	266.9 ± 11.31	19.91 ± 3.82	0.12 ± 0.03	193.2 ± 18.26	0.14 ± 0.03	0.04 ± 0.02
	p-Value		< 0.0001	0.03	0.1	0.32	0.95	0.22
Hindbrain	WT	4	89.08 ± 8.08	18.17 ± 1.99	n.d.	225.0 ± 7.200	0.55 ± 0.22	0.04 ± 0.02
	PDXP-KO	4	234.8 ± 14.02	44.23 ± 1.97	n.d.	234.5 ± 14.82	0.63 ± 0.08	0.07 ± 0.05
	p-Value		0.0001	< 0.0001	–	0.59	0.75	0.58
Cortex	WT	4	64.33 ± 3.89	13.16 ± 1.15	0.09 ± 0.03	145.1 ± 13.59	0.37 ± 0.09	0.007 ± 0.01
	PDXP-KO	4	250.8 ± 18.15	34.53 ± 3.07	0.16 ± 0.07	158.7 ± 10.24	0.38 ± 0.10	0.06 ± 0.03
	p-Value		< 0.0001	< 0.001	0.41	0.46	0.97	0.10
Midbrain	WT	4	85.41 ± 0.17	15.35 ± 1.25	0.06 ± 0.04	155.8 ± 15.03	0.39 ± 0.11	0.010 ± 0.004
	PDXP-KO	4	277.8 ± 6.02	43.18 ± 2.94	0.04 ± 0.04	191.1 ± 6.6	0.74 ± 0.17	0.11 ± 0.05
	p-Value		< 0.0001	0.0001	0.73	0.07	0.14	0.09
P6 brain	WT	4	95.25 ± 6.82	28.91 ± 1.21	0.07 ± 0.05	51.39 ± 4.98	0.17 ± 0.05	n.d.
	PDXP-KO	4	201.8 ± 3.97	48.00 ± 1.63	0.04 ± 0.04	53.53 ± 8.86	0.26 ± 0.03	0.01 ± 0.01
	p-Value		< 0.0001	< 0.0001	0.65	0.84	0.18	0.36

Shown are mean values ± S.E.M. *N* indicates the number of analyzed mice. For comparison with the other B_6 vitamers, results of the PLP measurements depicted in Fig. 3A and B are shown again here. Pyridoxine 5′-phosphate (PNP) could not be detected. Statistically significant differences between the two genotypes were analyzed using unpaired *t*-tests. Adult mice were 4 months-old males. P6, postnatal day 6; n.d., not detected.

concentrations were increased, we found that GAD67 expression was lowered by ~30% in PDXP-KO compared to WT brains, possibly as a result of a negative feedback response (Fig. 4D). GAD65 monomer or dimer levels were not detectably affected by the absence of PDXP expression. Interestingly, we observed a prominent high molecular weight (~220 kDa), GAD65-positive band in immunoblots of PDXP-KO brain lysates, which was only faintly visible in the controls (Fig. 4D). PLP-binding to GAD65 has profound effects on protein conformation [50,51], and elevated PLP levels might thereby favor the formation of SDS-resistant GAD65 complexes. Taken together, these data suggest that increased cellular PLP concentrations trigger holo-GAD65 formation, which augments synaptic GABA biosynthesis in PDXP-KO mouse brains.

GABA is involved in spatial learning behavior, for example by regulating adult hippocampal neurogenesis [52,53]. We therefore investigated the cognitive abilities of PDXP-KO mice in the Barnes maze. This task reports on hippocampus-dependent spatial reference memory by evaluating the ability to learn and remember the location of a hidden escape zone using a set of visual cues [54]. Fig. 5 demonstrates that PDXP-KO mice tended to require less time to locate the escape chamber (reduced target latency), and to search fewer holes before locating the escape chamber (less primary errors), but these trends did not reach statistical significance. However, PDXP-KO mice required significantly reduced path lengths (distances) to find the escape chamber compared to WT mice. PDXP-KO deletion also led to shorter escape latency, *i.e.* mice needed less time to enter the escape chamber. The analysis of reversal learning showed that PDXP-KO mice performed significantly better in terms of path length required to find the relocated escape chamber and escape latency (Fig. 5). Together, these results indicate that PDXP loss improved spatial learning and memory.

3.4. Anxiety-like behavior and impaired motor performance in PDXP-KO mice

Because of the important roles of GABA for neuronal activities involved in emotion, learning and memory, and the pivotal role of GABA for muscle tone and the regulation and execution of movements [55], we further examined PDXP-dependent mouse behavior and motor performance in a series of non-invasive tests. In the open field arena (a sensorimotor test used to assess general activity levels, locomotor activity and exploration), PDXP-KO mice spent less time in the center of the box. This difference was observed in 4–5 months old (young) and in 9–10 months old (middle-aged) mice (Fig. 6A). In the elevated plus maze (a test used to evaluate anxiety-related behavior), young PDXP-deficient mice behaved similar to WT controls, whereas middle-aged PDXP-KO mice entered the open arms less frequently and also stayed there for shorter times (Fig. 6B). Analysis of dark/light exploration showed a tendency towards anxiety-like behavior in PDXP-KO mice (as indicated by an increased latency to enter the lit compartment). However, this trend did not reach statistical significance; likewise, the time spent in the lit compartment was not different between WT and KO mice (Fig. 6C). Marble burying (a test that reports on anxiety-like, obsessive-compulsive, and repetitive behavior) increased in older PDXP-KO compared to age-matched WT mice (Fig. 6D). General locomotor activity (measured for all mice in parallel with the parameters shown in Fig. 6A–C) was not different between the two genotypes in these tasks. A sucrose preference test was conducted in 9 months-old male mice to evaluate anhedonia as an indicator of depressive-like behavior, yet no PDXP-dependent differences were observed (% sucrose intake relative to total fluid intake in mL: WT, 93.70 ± 2.08 mL, $n = 3$; KO, 88.70 ± 5.15 mL, $n = 3$; $p = 0.42$. Data are means ± S.E.M.). We conclude from these results that PDXP loss resulted in a mild, anxiety-like phenotype that was more prominent in middle-aged than in younger mice.

We next analyzed PDXP-dependent motor function. To exclude potential body weight differences as a confounding factor, we first compared the body weights of 4–5 months-old and 8–9 months-old male mice. There was a trend towards higher body weights in middle-aged, whole-body PDXP-KO mice, but this tendency did not reach statistical significance (4–5 months-old: WT, 29.64 ± 0.30 g, $n = 8$; PDXP-KO; 30.18 ± 1.06 g, $n = 8$, $p = 0.63$; 8–9 months-old: WT, 31.23 ± 0.63 g, $n = 12$; PDXP-KO, 33.36 ± 0.86 g, $n = 12$, $p = 0.06$. Data are means ± S.E.M.). The inverted screen test showed a significantly decreased performance of older PDXP-KO compared to WT mice (Fig. 7A). In the weights test, performance was already impaired in younger PDXP-KO mice (Fig. 7B; see Experimental Procedures for details). To evaluate muscle strength directly, we conducted grip strength measurements. Fore paw grip strength measurements in 8–9 months-old male mice did not show PDXP-dependent differences (WT 1.46 ± 0.04 N, $n = 12$; KO 1.42 ± 0.07 N, $n = 11$, $p = 0.61$). In contrast, hind paw grip strength measurements revealed poorer performance of PDXP-KO mice (WT 0.92 ± 0.02 N, $n = 8$; KO 0.77 ± 0.02 N, $n = 11$; $p < 0.0001$. Data for front and hind paw measurements are means ± S.E.M.).

PLP is a cofactor of glycogen phosphorylase, the enzyme that catalyzes the rate-limiting step in glycogenolysis. Because muscle glycogen is an important energy substrate during exercise, and PLP levels in skeletal muscle were significantly increased in PDXP-KO mice (see Fig. 3A), we asked whether PDXP loss in skeletal muscle or in the

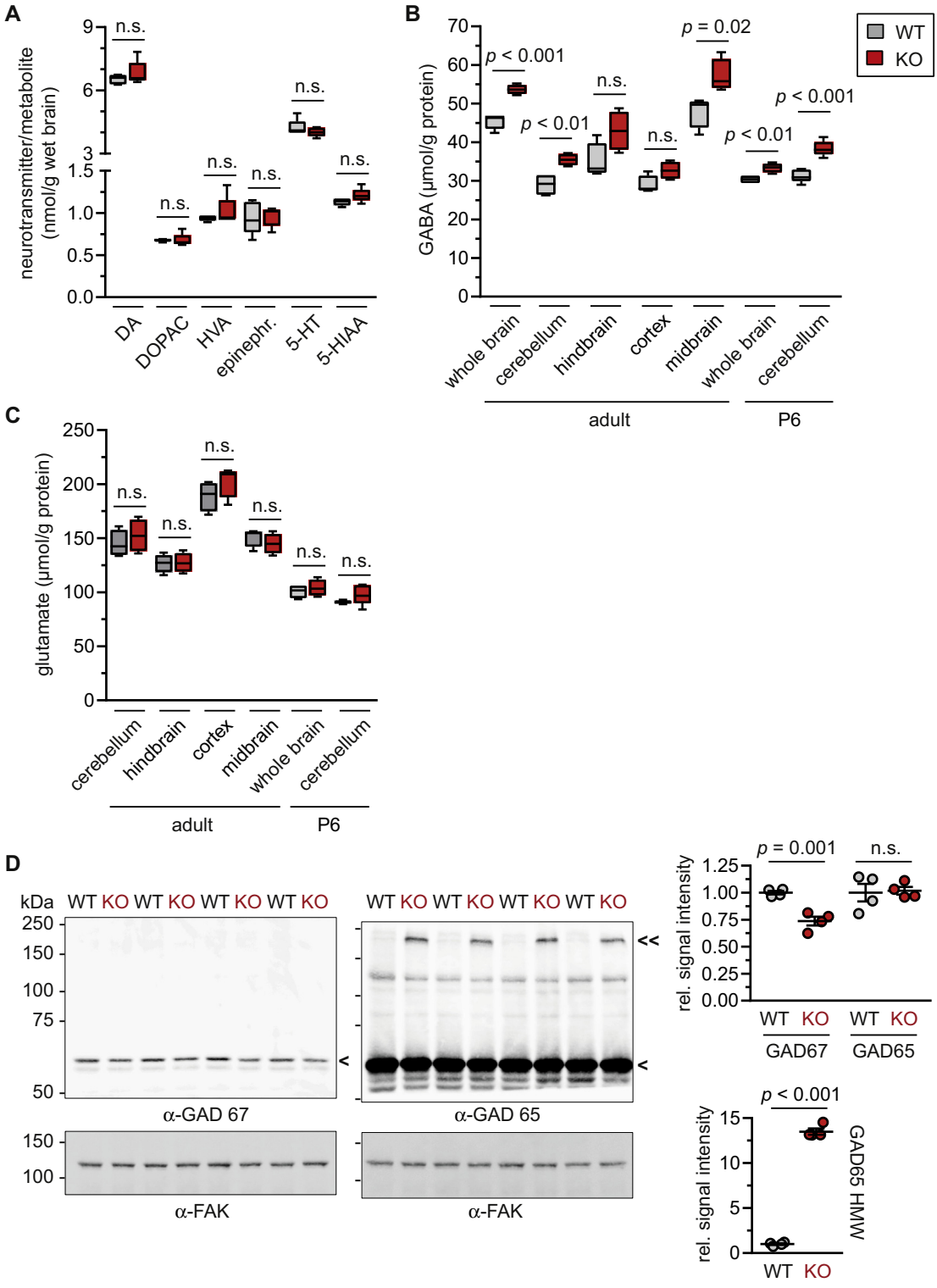

Fig. 4. Effect of whole-body PDXP deletion on neurotransmitter levels in the brain. (A) HPLC-based quantification of the indicated neurotransmitters and their catabolites in whole-brain extracts of 9 months-old male mice (n = 5 per genotype). DA, dopamine; DOPAC, 3,4-dihydroxyphenyl acetic acid; HVA, homovanillic acid; epinephr., epinephrine; 5-HT, 5-hydroxytryptamine (serotonin); 5-HIAA, 5-hydroxyindole acetic acid. (B) UPLC-MS/MS-based quantification of GABA levels in the brain. Whole brains were isolated from 8 months-old male mice (n = 4 per genotype). The indicated brain regions were dissected from 4 months-old male mice (n = 4 per genotype). P6, analysis of whole brains or dissected cerebellae from pups at postnatal day 6 (n = 4 per genotype). (C) UPLC-MS/MS-based quantification of glutamate levels in the brain. Samples were the same as those analyzed in (B). The whiskers indicate minimum and maximum values. (D) PDXP deficiency affects GAD67 and GAD65. Left and middle panels, GAD67 and GAD65 immunoblots. Brain lysates were generated from 8 months-old male mice, n = 4 per genotype. Focal adhesion kinase (FAK) served as a loading control. Blots were analyzed densitometrically, and GAD65/67 signals were normalized to FAK signals. The top right panel shows the quantification of GAD monomers (indicated by " < " in the blots), and the bottom right panel of the GAD65 high-molecular weight (HMW) complexes (indicated by " < < " in the blots). Note that all bands corresponding to GAD monomers and HMW complexes were analyzed densitometrically and are included in the figure, but that some symbols are overlapping and thus hidden. Data are mean values ± S.E.M.; n.s., non-significant. WT, wildtype mice; KO, *Pdxp*$^{flx/flx}$; *EIIa-Cre* mice.

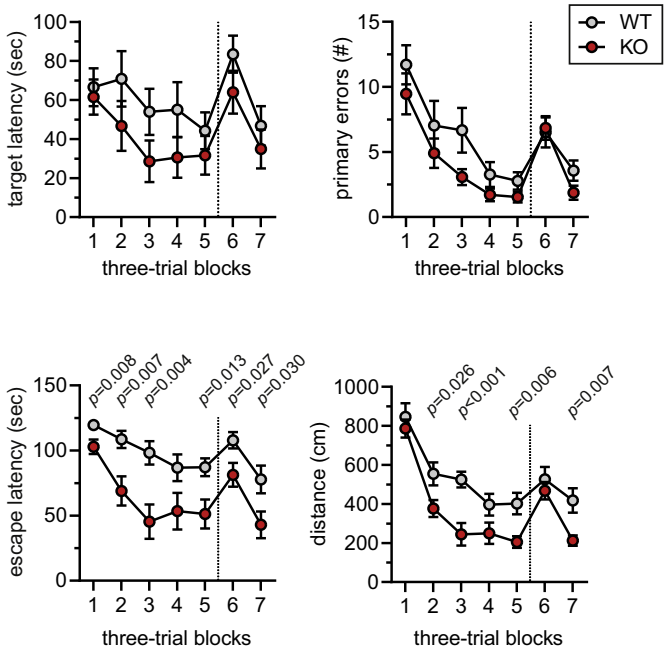

Fig. 5. Whole-body PDXP loss improves performance in the Barnes maze. Spatial learning and memory was assessed over five consecutive days, and three trials were performed per day ('three-trial blocks', shown as mean values ± S.E.M.). Afterwards, reversal learning was tested by moving the escape chamber to the opposite side of the maze (indicated by the vertical dotted line), and mice were analyzed for another two days in six additional trials. Scored parameters were target latency (time to locate the hole with the escape chamber), primary errors (number of holes searched before finding the hole equipped with the escape chamber), escape latency (time needed to enter the escape chamber) and distance (overall path length required before reaching the hole with the escape chamber). Tests were performed with $n = 12$ mice per genotype. All mice were 7 months-old males. Data are mean values ± S.E.M., *p*-values indicate statistically significant differences between WT and KO mice in each trial block. WT, wildtype mice; KO, *Pdxp*$^{flx/flx}$*; EIIa-Cre* mice.

nervous system was primarily responsible for the apparent motor impairments. To this end, mice deficient for PDXP either in skeletal muscle (*Pdxp*$^{flx/flx}$*; Acta1-Cre*$^{+/-}$; mKO) or in neural cells (*Pdxp*$^{flx/flx}$*; Nestin-Cre*$^{+/-}$; nKO) were generated. We verified efficient PDXP deletion in skeletal muscle and whole brain extracts in these two lines (Supplementary Fig. S2A, B). Because of the known metabolic issues related to knockouts driven by Nestin-Cre [56], mice with a neural cell-directed PDXP deletion were only characterized at 4–5 months of age. PDXP deletion in neural cells led to an increase in whole brain PLP levels (Supplementary Fig. S2C). Although there was a tendency towards increased GABA concentrations in nKO mice, these changes were statistically non-significant (Supplementary Fig. S2D). Similar to brain extracts generated from whole-body PDXP-KO mice (see Fig. 4D), we detected a high molecular weight, GAD65-positive band in immunoblots of nKO brain lysates (Supplementary Fig. S2E). These results suggest that the appearance of high molecular weight GAD65 complexes is a sensitive indicator of increased PLP levels, and that cell types other than neurons, for example glial and endothelial cells [57] contribute to the overall regulation of GABA levels in whole-body PDXP-KO mice.

Grip strength measurements in young mice showed that PDXP ablation in neural cells significantly reduced hind paw strength, whereas PDXP loss in skeletal muscle increased hind paw strength in older mice (Fig. 7C). Hence, PDXP deficiency in skeletal muscle does not account for the decreased grip strength of globally PDXP-deficient mice. We conclude that a dominant loss of PDXP function in another organ, most likely the brain, causes the decrease in neuromuscular strength observed in whole-body PDXP-KO mice.

4. Discussion

We demonstrate that PDXP (also known as PLPP, chronophin or CIN) is a major regulator of PLP concentrations *in vivo*, and that whole-body PDXP ablation elevates PLP and GABA levels in the brain.

Spatial learning and memory was improved in PDXP-deficient compared to WT mice, and GABA may be involved in this behavior. Many neuropsychiatric disorders and neurodegenerative diseases encompass dysfunctional GABA system components, and the disruption of GABAergic inhibitory circuits with a resulting excitatory/inhibitory imbalance is likely to contribute to some of the clinical features of these disorders [58–60]. GABA signaling is also impaired in the aged hippocampus, suggesting that pharmacological strategies might improve memory function and spatial navigation abilities in the elderly population [61,62]. A recent neuroimaging study that investigated the association between vitamin B6 blood levels and cognition, brain structure and functional connectivity in healthy older humans (N > 600; age range 55–85 years) has shown that vitamin B6 supplementation was positively related to cortical folding and thus to the preservation of brain structure. However, neuropsychological testing did not detect an improvement in cognitive performance, and only slight changes in functional connectivity were found [63]. Based on these data, the authors hypothesized that vitamin B6 might counteract the gray matter loss that frequently occurs in older age, and stabilize cognitive abilities.

A meta-analysis of brain GABA levels in different neuropsychiatric diseases has revealed a GABAergic deficit in the brains of subjects with autism spectrum disorders and major depression [64], and subtype-selective GABA-A receptor modulators show potential as novel antidepressants [65,66]. GABA concentrations below a certain threshold lead to seizures, and a number of anti-epileptic drugs target the GABAergic system [67]. GABA levels are determined by GABA biosynthesis *via* PLP-dependent glutamic acid decarboxylases, and GABA catabolism through the PLP-dependent GABA transaminase. The selective GABA transaminase suicide inhibitor vigabatrin [68] increases GABA levels, and is used for the treatment of infantile spasms and as an adjunctive therapy for refractory and complex partial seizures in adults [69,70]. Despite its clinical efficacy, vigabatrin therapy is associated with harmful side effects, such as the dose-dependent risk for progressive and permanent visual field defects [69,70]. It is tempting to speculate that a combination of a pharmacological PDXP inhibitor together with vigabatrin may further increase GABA levels in the brain and allow for a vigabatrin dose reduction.

The anxiety-like phenotype of PDXP-KO mice was unexpected, given the physiological role of GABA in counteracting anxiety *via* GABA-A receptors [58,65,66]. However, PLP and GABA levels were already elevated postnatally in our mouse model. GABA levels affect brain development [71] and synaptogenesis [72], and can thereby impact stress responses later in life. For example, postnatal administration of the GABA-A receptor agonist muscimol results in anxiety-like behavior in 3-months old mice [73]. The EIIa-Cre driven, embryonic ablation of PDXP might affect brain development (through GABA and/or other mechanisms), and influence stress susceptibility and anxiety in that way. PDXP loss might also alter the balance between excitatory and inhibitory transmission in specific synapses in the adult organism. For example, GABA co-released with glutamate controls the activity of the lateral habenula, a region in the dorsal thalamus that regulates mood and anxiety [74]. Finally, we found elevated D/L-serine levels (stereoisomers were not resolved in our analysis) in the cortex, and decreased glycine concentrations in the hindbrains of PDXP-KO mice. Serine racemase is a PLP-dependent enzyme, and D-serine is a co-agonist at *N*-methyl-D-aspartic acid (NMDA) glutamate receptors in the brain. Glycine acts as an inhibitory neurotransmitter in the spinal cord and brainstem, and has excitatory effects in the cerebral cortex due to its agonistic activity at glutamatergic NMDA receptors. These changes may contribute to the observed behavioral phenotypes. Further work is necessary to investigate the electrophysiological consequences of PDXP

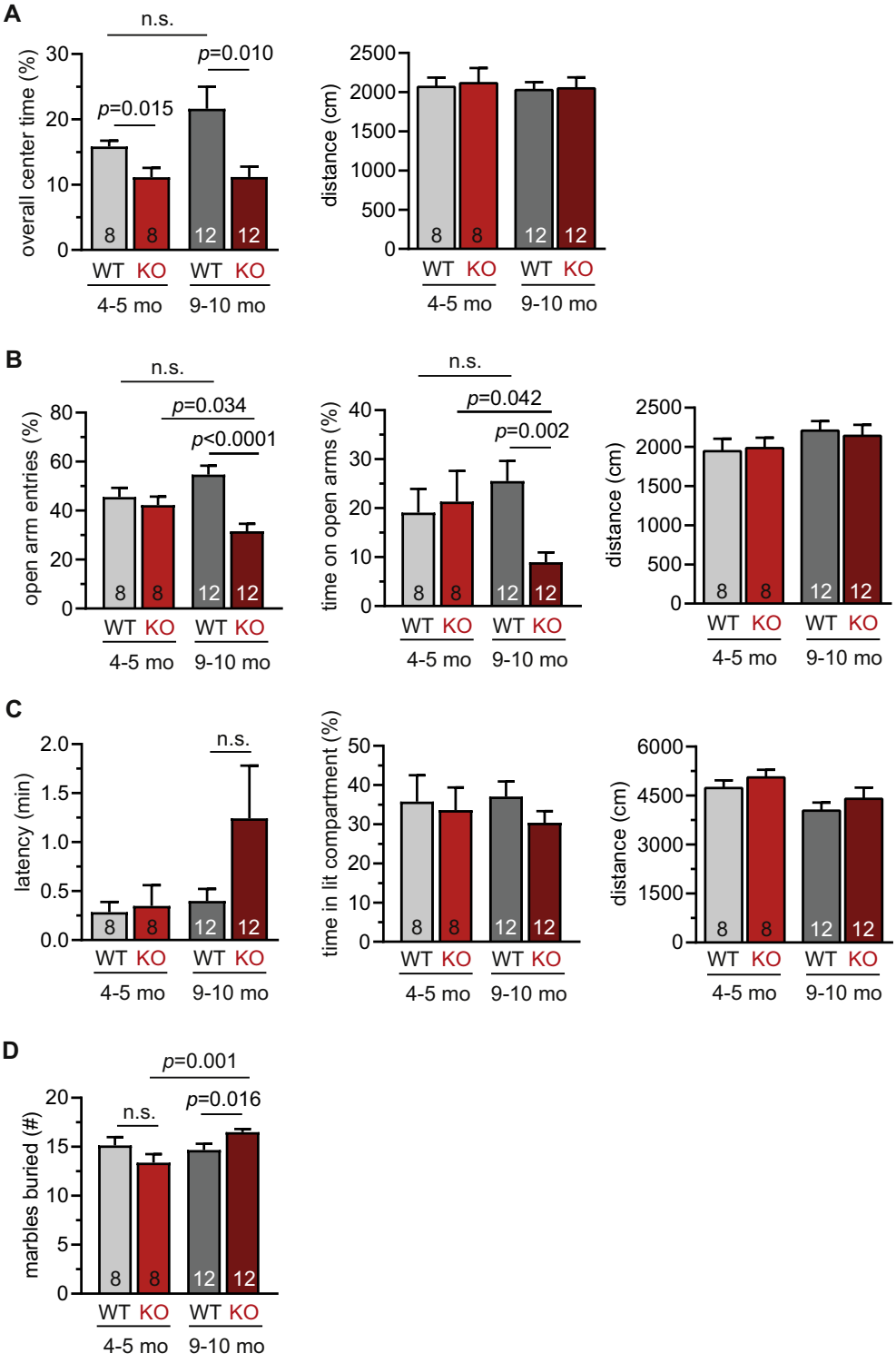

Fig. 6. Whole-body PDXP loss results in a mild anxiety-like behavior. (A) Open field test. Scored parameters were time in the center of the open field arena and overall locomotion (horizontal distance covered in the 30 min test period). (B) Elevated plus maze. Open arm entries, time on open arms and overall locomotion were scored during the 10 min test period. (C) Dark/light box. The latency to enter and the time spent in the lit compartment was measured together with the overall locomotion in the 10 min test period. (D) Marble burying. The number of marbles buried within the 30 min test period was counted. Mo, months. Data are mean values + S.E.M. The number of analyzed mice is indicated in the bars. WT, wildtype mice; KO, *Pdxp*$^{flx/flx}$; *EIIa-Cre* mice.

loss in specific brain regions and synapses, and to characterize the involved receptors and signaling pathways in our mouse model [75].

In addition to a GABA-dependent decrease in muscle tone [76], the apparent motor deficits of PDXP-KO mice might be influenced by increased anxiety. In addition, age-dependent processes related to continuously elevated cellular PLP levels may contribute to the observed phenotype. An increased anxiety-like behavior could add to the retardation of spatial learning that was observed when PLPP/CIN (PDXP)-deficient mice were tested in the Morris water maze in another study [37]. The water maze imposes a much stronger aversive stimulus and more stressful conditions on mice than the dry-land Barnes maze used in our study, and increased stress and anxiety may confound the assay outcome [54]. The discrepant results obtained in the two PDXP-KO mouse models might also be linked to differences in the analyzed mouse strains, as well as in animal age, -sex or -housing conditions. The mice investigated in our present study were conditionally PDXP-deficient males of the indicated ages; animals were on a C57BL/6J background and maintained under specific pathogen-free conditions. Kim et al. have described mice with a constitutive PDXP knockout on a mixed 129/SvEv-C57BL/6J albino background; age, sex and housing conditions of the animals were not

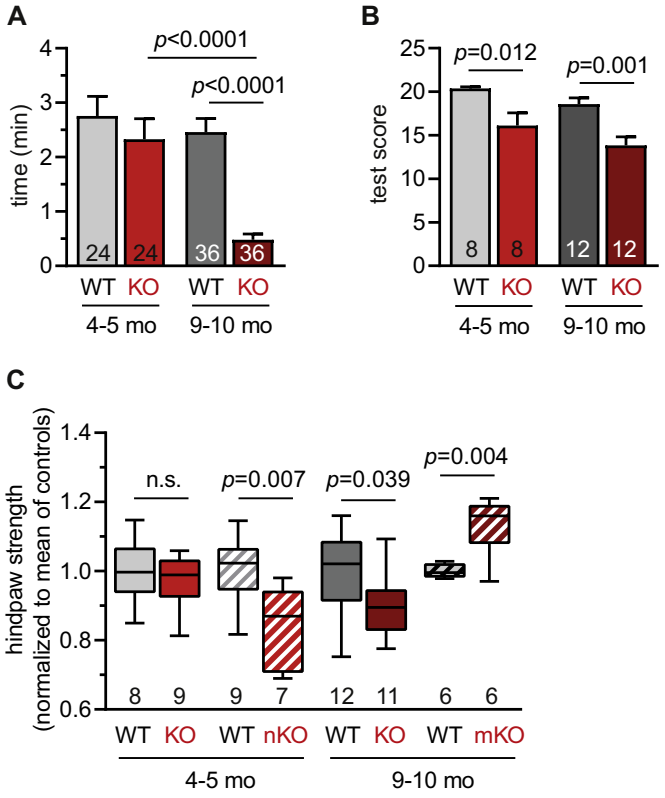

Fig. 7. PDXP loss impairs motor performance and reduces muscle strength. (A) Inverted screen test. Latency to fall off the grid into the cage was measured. (B) Weights test. The test score represents the number of chain links the mice lifted for 3 s, multiplied by the time the weight was held in sec. Data in (A) and (B) are mean values + S.E.M. (C) Hind paw grip strength measurements. Grip strengths were normalized to the mean values of the respective control cohorts. The whiskers show minimum and maximum values; the median value is indicated in the box. The number of analyzed mice are given in the bars or underneath the box plots. KO, whole-body PDXP-KO; nKO, neural cell-specific PDXP-KO; mKO, skeletal muscle-specific PDXP-KO. All animals were males; WT signifies floxed littermate controls (for nKO and mKO mice) or WT mice (for whole-body KO). Mo, months; n.s., non-significant.

reported [37]. The inbred strain background can impact behavioral measures, and learning and memory is an age-dependent process [77–79].

Previous work by us and others has investigated the cofilin regulatory function of PDXP [31–36], and a recent study has reported effects of PDXP on hippocampal cofilin phosphoregulation *in vivo* [37]. Yet, a direct cofilin phosphatase activity of PDXP is difficult to reconcile with crystallographic work from different laboratories, including our own [21,38,80] (Protein Data Bank entries 2OYC, 2P69, 2P27, 2CFR, 2CFS, 2CFT, 5GYN, 4BX3, 4BXO, 4BX2, 4BKM, 5AES). PLP is deeply buried within the catalytic cleft of PDXP [80], and the active site is occluded by a large capping domain typical of small molecule-directed, haloacid dehalogenase (HAD)-type hydrolases [81,82]. Given these structural features, extensive conformational changes would be required to accommodate a protein substrate. Without structural information on the mechanism of cofilin dephosphorylation by PDXP, it currently appears more likely that the effects of PDXP on phosphocofilin that are found in some studies are caused by indirect mechanisms.

Supplementary data to this article can be found online at https://doi.org/10.1016/j.bbadis.2018.08.018.

Transparency document

The Transparency document associated this article can be found, in online version.

Acknowledgements

We thank Angelika Keller and Kerstin Hadamek for excellent technical assistance, and Heinrich Blazyca and Drs. Dennis Klein and Rudolf Martini for generous help with grip strength measurements. Marjolein Bosma is thanked for the analysis of B6 vitamers. We acknowledge the assistance of Charlotte Auth and Gabriel Christmann with immunoblots. This work was supported by the Deutsche Forschungsgemeinschaft SFB728 and SFB688 (to AG) and the IZKF Würzburg (to LH). CW was supported by a predoctoral fellowship from the Medical Faculty of the University of Würzburg (Graduate School of Life Sciences) and by a Kaltenbach predoctoral fellowship from the German Heart Foundation.

References

[1] R. Percudani, A. Peracchi, A genomic overview of pyridoxal-phosphate-dependent enzymes, EMBO Rep. 4 (2003) 850–854.
[2] J.P. Richard, T.L. Amyes, J. Crugeiras, A. Rios, Pyridoxal 5′-phosphate: electrophilic catalyst extraordinaire, Curr. Opin. Chem. Biol. 13 (2009) 475–483.
[3] M.L. di Salvo, R. Contestabile, M.K. Safo, Vitamin B(6) salvage enzymes: mechanism, structure and regulation, Biochim. Biophys. Acta 1814 (2011) 1597–1608.
[4] N. Darin, E. Reid, L. Prunetti, L. Samuelsson, R.A. Husain, M. Wilson, B. El Yacoubi, E. Footitt, W.K. Chong, L.C. Wilson, H. Prunty, S. Pope, S. Heales, K. Lascelles, M. Champion, E. Wassmer, P. Veggiotti, V. de Crecy-Lagard, P.B. Mills, P.T. Clayton, Mutations in PROSC disrupt cellular pyridoxal phosphate homeostasis and cause vitamin-B6-dependent epilepsy, Am. J. Hum. Genet. 99 (2016) 1325–1337.
[5] J.W. Whittaker, Intracellular trafficking of the pyridoxal cofactor. Implications for health and metabolic disease, Arch. Biochem. Biophys. 592 (2016) 20–26.
[6] M. Albersen, M. Bosma, N.V. Knoers, B.H. de Ruiter, E.F. Diekman, J. de Ruijter, W.F. Visser, T.J. de Koning, N.M. Verhoeven-Duif, The intestine plays a substantial role in human vitamin B6 metabolism: a Caco-2 cell model, PLoS One 8 (2013) e54113.
[7] M.L. Fonda, Purification and characterization of vitamin B6-phosphate phosphatase from human erythrocytes, J. Biol. Chem. 267 (1992) 15978–15983.
[8] Y.M. Jang, D.W. Kim, T.C. Kang, M.H. Won, N.I. Baek, B.J. Moon, S.Y. Choi, O.S. Kwon, Human pyridoxal phosphatase. Molecular cloning, functional expression, and tissue distribution, J. Biol. Chem. 278 (2003) 50040–50046.
[9] M.L. di Salvo, M.K. Safo, R. Contestabile, Biomedical aspects of pyridoxal 5′-phosphate availability, Front. Biosci. (Elite Ed.) 4 (2012) 897–913.
[10] P. Zhang, K. Tsuchiya, T. Kinoshita, H. Kushiyama, S. Suidasari, M. Hatakeyama, H. Imura, N. Kato, T. Suda, Vitamin B6 prevents IL-1beta protein production by inhibiting NLRP3 inflammasome activation, J. Biol. Chem. 291 (2016) 24517–24527.
[11] P.M. Ueland, A. McCann, O. Midttun, A. Ulvik, Inflammation, vitamin B6 and related pathways, Mol. Asp. Med. 53 (2017) 10–27.
[12] P.T. Clayton, B6-responsive disorders: a model of vitamin dependency, J. Inherit. Metab. Dis. 29 (2006) 317–326.
[13] P.B. Mills, E. Struys, C. Jakobs, B. Plecko, P. Baxter, M. Baumgartner, M.A. Willemsen, H. Omran, U. Tacke, B. Uhlenberg, B. Weschke, P.T. Clayton, Mutations in antiquitin in individuals with pyridoxine-dependent seizures, Nat. Med. 12 (2006) 307–309.
[14] P.B. Mills, R.A. Surtees, M.P. Champion, C.E. Beesley, N. Dalton, P.J. Scambler, S.J. Heales, A. Briddon, I. Scheimberg, G.F. Hoffmann, J. Zschocke, P.T. Clayton, Neonatal epileptic encephalopathy caused by mutations in the PNPO gene encoding pyridox(am)ine 5′-phosphate oxidase, Hum. Mol. Genet. 14 (2005) 1077–1086.
[15] G.F. Hoffmann, B. Schmitt, M. Windfuhr, N. Wagner, H. Strehl, S. Bagci, A.R. Franz, P.B. Mills, P.T. Clayton, M.R. Baumgartner, B. Steinmann, T. Bast, N.I. Wolf, J. Zschocke, Pyridoxal 5′-phosphate may be curative in early-onset epileptic encephalopathy, J. Inherit. Metab. Dis. 30 (2007) 96–99.
[16] M. Albersen, M. Bosma, J.J. Jans, F.C. Hofstede, P.M. van Hasselt, M.G. de Sain-van der Velden, G. Visser, N.M. Verhoeven-Duif, Vitamin B6 in plasma and cerebrospinal fluid of children, PLoS One 10 (2015) e0120972.
[17] B. Plecko, M. Zweier, A. Begemann, D. Mathis, B. Schmitt, P. Striano, M. Baethmann, M.S. Vari, F. Beccaria, F. Zara, L.M. Crowther, P. Joset, H. Sticht, S.M. Papuc, A. Rauch, Confirmation of mutations in PROSC as a novel cause of vitamin B6-dependent epilepsy, J. Med. Genet. 54 (2017) 809–814.
[18] H. Schaumburg, J. Kaplan, A. Windebank, N. Vick, S. Rasmus, D. Pleasure, M.J. Brown, Sensory neuropathy from pyridoxine abuse. A new megavitamin syndrome, N. Engl. J. Med. 309 (1983) 445–448.
[19] K. Dalton, M.J. Dalton, Characteristics of pyridoxine overdose neuropathy syndrome, Acta Neurol. Scand. 76 (1987) 8–11.
[20] S.M. Gospe Jr., M.P. Adam, H.H. Ardinger, R.A. Pagon, S.E. Wallace, L.J.H. Bean, K. Stephens, A. Amemiya (Eds.), Pyridoxine-dependent Epilepsy, GeneReviews®, Seattle (WA), 1993.
[21] G. Knobloch, N. Jabari, S. Stadlbauer, H. Schindelin, M. Kohn, A. Gohla, Synthesis of hydrolysis-resistant pyridoxal 5′-phosphate analogs and their biochemical and X-ray crystallographic characterization with the pyridoxal phosphatase chronophin, Bioorg. Med. Chem. 23 (2015) 2819–2827.
[22] H. Prinsen, B.G.M. Schiebergen-Bronkhorst, M.W. Roeleveld, J.J.M. Jans, M.G.M. de Sain-van der Velden, G. Visser, P.M. van Hasselt, N.M. Verhoeven-Duif,

Rapid quantification of underivatized amino acids in plasma by hydrophilic interaction liquid chromatography (HILIC) coupled with tandem mass-spectrometry, J. Inherit. Metab. Dis. 39 (2016) 651–660.
[23] R.R. Schur, M.P. Boks, E. Geuze, H.C. Prinsen, N.M. Verhoeven-Duif, M. Joels, R.S. Kahn, E. Vermetten, C.H. Vinkers, Development of psychopathology in deployed armed forces in relation to plasma GABA levels, Psychoneuroendocrinology 73 (2016) 263–270.
[24] M. van der Ham, M. Albersen, T.J. de Koning, G. Visser, A. Middendorp, M. Bosma, N.M. Verhoeven-Duif, M.G. de Sain-van der Velden, Quantification of vitamin B6 vitamers in human cerebrospinal fluid by ultra performance liquid chromatography-tandem mass spectrometry, Anal. Chim. Acta 712 (2012) 108–114.
[25] A. Raab, S. Popp, K.P. Lesch, M.J. Lohse, M. Fischer, J. Deckert, L. Hommers, Increased fear learning, spatial learning as well as neophobia in Rgs2(−/−) mice, Genes Brain Behav. 17 (2018) e12420.
[26] R.M. Deacon, Digging and marble burying in mice: simple methods for in vivo identification of biological impacts, Nat. Protoc. 1 (2006) 122–124.
[27] T. Strekalova, R. Spanagel, D. Bartsch, F.A. Henn, P. Gass, Stress-induced anhedonia in mice is associated with deficits in forced swimming and exploration, Neuropsychopharmacology 29 (2004) 2007–2017.
[28] M.Y. Liu, C.Y. Yin, L.J. Zhu, X.H. Zhu, C. Xu, C.X. Luo, H. Chen, D.Y. Zhu, Q.G. Zhou, Sucrose preference test for measurement of stress-induced anhedonia in mice, Nat. Protoc. 13 (2018) 1686–1698.
[29] R.M. Deacon, Measuring the strength of mice, J. Vis. Exp. 76 (2013), https://doi.org/10.3791/2610.
[30] B. Kohl, S. Fischer, J. Groh, C. Wessig, R. Martini, MCP-1/CCL2 modifies axon properties in a PMP22-overexpressing mouse model for Charcot-Marie-tooth 1A neuropathy, Am. J. Pathol. 176 (2010) 1390–1399.
[31] A. Gohla, J. Birkenfeld, G.M. Bokoch, Chronophin, a novel HAD-type serine protein phosphatase, regulates cofilin-dependent actin dynamics, Nat. Cell Biol. 7 (2005) 21–29.
[32] M. Schulze, O. Fedorchenko, T.G. Zink, C.B. Knobbe-Thomsen, S. Kraus, S. Schwinn, A. Beilhack, G. Reifenberger, C.M. Monoranu, A.L. Siren, E. Jeanclos, A. Gohla, Chronophin is a glial tumor modifier involved in the regulation of glioblastoma growth and invasiveness, Oncogene 35 (2016) 3163–3177.
[33] V. Delorme-Walker, J.Y. Seo, A. Gohla, B. Fowler, B. Bohl, C. DerMardirossian, Chronophin coordinates cell leading edge dynamics by controlling active cofilin levels, Proc. Natl. Acad. Sci. U. S. A. 112 (2015) E5150–E5159.
[34] C.X. Sun, M.A. Magalhaes, M. Glogauer, Rac1 and Rac2 differentially regulate actin free barbed end formation downstream of the fMLP receptor, J. Cell Biol. 179 (2007) 239–245.
[35] M. Zoudilova, P. Kumar, L. Ge, P. Wang, G.M. Bokoch, K.A. DeFea, Beta-arrestin-dependent regulation of the cofilin pathway downstream of protease-activated receptor-2, J. Biol. Chem. 282 (2007) 20634–20646.
[36] T.Y. Huang, L.S. Minamide, J.R. Bamburg, G.M. Bokoch, Chronophin mediates an ATP-sensing mechanism for cofilin dephosphorylation and neuronal cofilin-actin rod formation, Dev. Cell 15 (2008) 691–703.
[37] J.E. Kim, Y.J. Kim, D.S. Lee, J.Y. Kim, A.R. Ko, H.W. Hyun, M.J. Kim, T.C. Kang, PLPP/CIN regulates bidirectional synaptic plasticity via GluN2A interaction with postsynaptic proteins, Sci. Rep. 6 (2016) 26576.
[38] C. Kestler, G. Knobloch, I. Tessmer, E. Jeanclos, H. Schindelin, A. Gohla, Chronophin dimerization is required for proper positioning of its substrate specificity loop, J. Biol. Chem. 289 (2014) 3094–3103.
[39] S.P. Coburn, Vitamin B-6 metabolism and interactions with TNAP, Subcell. Biochem. 76 (2015) 207–238.
[40] H. Mehansho, M.W. Hamm, L.M. Henderson, Transport and metabolism of pyridoxal and pyridoxal phosphate in the small intestine of the rat, J. Nutr. 109 (1979) 1542–1551.
[41] M.P. Whyte, J.D. Mahuren, L.A. Vrabel, S.P. Coburn, Markedly increased circulating pyridoxal-5′-phosphate levels in hypophosphatasia. Alkaline phosphatase acts in vitamin B6 metabolism, J. Clin. Invest. 76 (1985) 752–756.
[42] K.G. Waymire, J.D. Mahuren, J.M. Jaje, T.R. Guilarte, S.P. Coburn, G.R. MacGregor, Mice lacking tissue non-specific alkaline phosphatase die from seizures due to defective metabolism of vitamin B-6, Nat. Genet. 11 (1995) 45–51.
[43] H. Zimmermann, D. Langer, Tissue-nonspecific alkaline phosphatase in the developing brain and in adult neurogenesis, Subcell. Biochem. 76 (2015) 61–84.
[44] M.K. Rahman, T. Nagatsu, T. Sakurai, S. Hori, M. Abe, M. Matsuda, Effect of pyridoxal phosphate deficiency on aromatic L-amino acid decarboxylase activity with L-DOPA and L-5-hydroxytryptophan as substrates in rats, Jpn. J. Pharmacol. 32 (1982) 803–811.
[45] E. Roberts, K. Kuriyama, Biochemical-physiological correlations in studies of the gamma-aminobutyric acid system, Brain Res. 8 (1968) 1–35.
[46] D.L. Martin, K. Rimvall, Regulation of gamma-aminobutyric acid synthesis in the brain, J. Neurochem. 60 (1993) 395–407.
[47] D.F. Bu, M.G. Erlander, B.C. Hitz, N.J. Tillakaratne, D.L. Kaufman, C.B. Wagner-McPherson, G.A. Evans, A.J. Tobin, Two human glutamate decarboxylases, 65-kDa GAD and 67-kDa GAD, are each encoded by a single gene, Proc. Natl. Acad. Sci. U. S. A. 89 (1992) 2115–2119.
[48] J.J. Soghomonian, D.L. Martin, Two isoforms of glutamate decarboxylase: why? Trends Pharmacol. Sci. 19 (1998) 500–505.
[49] C.S. Pinal, A.J. Tobin, Uniqueness and redundancy in GABA production, Perspect. Dev. Neurobiol. 5 (1998) 109–118.
[50] I. Kass, D.E. Hoke, M.G. Costa, C.F. Reboul, B.T. Porebski, N.P. Cowieson, H. Leh, E. Pennacchietti, J. McCoey, O. Kleifeld, C. Borri Voltattorni, D. Langley, B. Roome, I.R. Mackay, D. Christ, D. Perahia, M. Buckle, A. Paiardini, D. De Biase, A.M. Buckle, Cofactor-dependent conformational heterogeneity of GAD65 and its role in autoimmunity and neurotransmitter homeostasis, Proc. Natl. Acad. Sci. U. S. A. 111 (2014) E2524–E2529.
[51] G. Giardina, R. Montioli, S. Gianni, B. Cellini, A. Paiardini, C.B. Voltattorni, F. Cutruzzola, Open conformation of human DOPA decarboxylase reveals the mechanism of PLP addition to Group II decarboxylases, Proc. Natl. Acad. Sci. U. S. A. 108 (2011) 20514–20519.
[52] C. Lieberwirth, Y. Pan, Y. Liu, Z. Zhang, Z. Wang, Hippocampal adult neurogenesis: its regulation and potential role in spatial learning and memory, Brain Res. 1644 (2016) 127–140.
[53] S. Ge, D.A. Pradhan, G.L. Ming, H. Song, GABA sets the tempo for activity-dependent adult neurogenesis, Trends Neurosci. 30 (2007) 1–8.
[54] F.E. Harrison, A.H. Hosseini, M.P. McDonald, Endogenous anxiety and stress responses in water maze and Barnes maze spatial memory tasks, Behav. Brain Res. 198 (2009) 247–251.
[55] U. Rudolph, H. Mohler, Analysis of GABAA receptor function and dissection of the pharmacology of benzodiazepines and general anesthetics through mouse genetics, Annu. Rev. Pharmacol. Toxicol. 44 (2004) 475–498.
[56] J. Declercq, B. Brouwers, V.P. Pruniau, P. Stijnen, G. de Faudeur, K. Tuand, S. Meulemans, L. Serneels, A. Schraenen, F. Schuit, J.W. Creemers, Metabolic and behavioural phenotypes in Nestin-Cre mice are caused by hypothalamic expression of human growth hormone, PLoS One 10 (2015) e0135502.
[57] S. Li, T.P. Kumar, S. Joshee, T. Kirschstein, S. Subburaju, J.S. Khalili, J. Kloepper, C. Du, A. Elkhal, G. Szabo, R.K. Jain, R. Kohling, A. Vasudevan, Endothelial cell-derived GABA signaling modulates neuronal migration and postnatal behavior, Cell Res. 28 (2018) 221–248.
[58] U. Rudolph, H. Mohler, GABAA receptor subtypes: therapeutic potential in Down syndrome, affective disorders, schizophrenia, and autism, Annu. Rev. Pharmacol. Toxicol. 54 (2014) 483–507.
[59] O. Marin, Interneuron dysfunction in psychiatric disorders, Nat. Rev. Neurosci. 13 (2012) 107–120.
[60] B. Luscher, Q. Shen, N. Sahir, The GABAergic deficit hypothesis of major depressive disorder, Mol. Psychiatry 16 (2011) 383–406.
[61] J.A. McQuail, C.J. Frazier, J.L. Bizon, Molecular aspects of age-related cognitive decline: the role of GABA signaling, Trends Mol. Med. 21 (2015) 450–460.
[62] A. Rozycka, M. Liguz-Lecznar, The space where aging acts: focus on the GABAergic synapse, Aging Cell 16 (2017) 634–643.
[63] K. Jannusch, C. Jockwitz, H.J. Bidmon, S. Moebus, K. Amunts, S. Caspers, A complex interplay of vitamin B1 and B6 metabolism with cognition, brain structure, and functional connectivity in older adults, Front. Neurosci. 11 (2017) 596.
[64] R.R. Schur, L.W. Draisma, J.P. Wijnen, M.P. Boks, M.G. Koevoets, M. Joels, D.W. Klomp, R.S. Kahn, C.H. Vinkers, Brain GABA levels across psychiatric disorders: a systematic literature review and meta-analysis of (1) H-MRS studies, Hum. Brain Mapp. 37 (2016) 3337–3352.
[65] H. Mohler, The GABA system in anxiety and depression and its therapeutic potential, Neuropharmacology 62 (2012) 42–53.
[66] K.S. Smith, U. Rudolph, Anxiety and depression: mouse genetics and pharmacological approaches to the role of GABA(A) receptor subtypes, Neuropharmacology 62 (2012) 54–62.
[67] M. Bialer, H.S. White, Key factors in the discovery and development of new antiepileptic drugs, Nat. Rev. Drug Discov. 9 (2010) 68–82.
[68] B. Lippert, B.W. Metcalf, M.J. Jung, P. Casara, 4-Amino-hex-5-enoic acid, a selective catalytic inhibitor of 4-aminobutyric-acid aminotransferase in mammalian brain, Eur. J. Biochem. 74 (1977) 441–445.
[69] W.D. Shields, J.M. Pellock, Vigabatrin 35 years later - from mechanism of action to benefit-risk considerations, Acta Neurol. Scand. Suppl. (2011) 1–4.
[70] E. Ben-Menachem, Mechanism of action of vigabatrin: correcting misperceptions, Acta Neurol. Scand. Suppl. (2011) 5–15.
[71] A. Represa, Y. Ben-Ari, Trophic actions of GABA on neuronal development, Trends Neurosci. 28 (2005) 278–283.
[72] W.C. Oh, S. Lutzu, P.E. Castillo, H.B. Kwon, De novo synaptogenesis induced by GABA in the developing mouse cortex, Science 353 (2016) 1037–1040.
[73] A.A. Salari, A. Bakhtiari, J.R. Homberg, Activation of GABA-A receptors during postnatal brain development increases anxiety- and depression-related behaviors in a time- and dose-dependent manner in adult mice, Eur. Neuropsychopharmacol. 25 (2015) 1260–1274.
[74] S.J. Shabel, C.D. Proulx, J. Piriz, R. Malinow, Mood regulation. GABA/glutamate co-release controls habenula output and is modified by antidepressant treatment, Science 345 (2014) 1494–1498.
[75] M. Farrant, Z. Nusser, Variations on an inhibitory theme: phasic and tonic activation of GABA(A) receptors, Nat. Rev. Neurosci. 6 (2005) 215–229.
[76] F. Crestani, K. Low, R. Keist, M. Mandelli, H. Mohler, U. Rudolph, Molecular targets for the myorelaxant action of diazepam, Mol. Pharmacol. 59 (2001) 442–445.
[77] J.N. Crawley, J.K. Belknap, A. Collins, J.C. Crabbe, W. Frankel, N. Henderson, R.J. Hitzemann, S.C. Maxson, L.L. Miner, A.J. Silva, J.M. Wehner, A. Wynshaw-Boris, R. Paylor, Behavioral phenotypes of inbred mouse strains: implications and recommendations for molecular studies, Psychopharmacology 132 (1997) 107–124.
[78] K.R. Bailey, N.R. Rustay, J.N. Crawley, Behavioral phenotyping of transgenic and knockout mice: practical concerns and potential pitfalls, ILAR J. 47 (2006) 124–131.

[79] I. Schneider, W.S. Tirsch, T. Faus-Kessler, L. Becker, E. Kling, R.L. Busse, A. Bender, B. Feddersen, J. Tritschler, H. Fuchs, V. Gailus-Durner, K.H. Englmeier, M.H. de Angelis, T. Klopstock, Systematic, standardized and comprehensive neurological phenotyping of inbred mice strains in the German Mouse Clinic, J. Neurosci. Methods 157 (2006) 82–90.

[80] S.C. Almo, J.B. Bonanno, J.M. Sauder, S. Emtage, T.P. Dilorenzo, V. Malashkevich, S.R. Wasserman, S. Swaminathan, S. Eswaramoorthy, R. Agarwal, D. Kumaran, M. Madegowda, S. Ragumani, Y. Patskovsky, J. Alvarado, U.A. Ramagopal, J. Faber-Barata, M.R. Chance, A. Sali, A. Fiser, Z.Y. Zhang, D.S. Lawrence, S.K. Burley, Structural genomics of protein phosphatases, J. Struct. Funct. Genom. 8 (2007) 121–140.

[81] A. Seifried, J. Schultz, A. Gohla, Human HAD phosphatases: structure, mechanism, and roles in health and disease, FEBS J. 280 (2013) 549–571.

[82] A.M. Burroughs, K.N. Allen, D. Dunaway-Mariano, L. Aravind, Evolutionary genomics of the HAD superfamily: understanding the structural adaptations and catalytic diversity in a superfamily of phosphoesterases and allied enzymes, J. Mol. Biol. 361 (2006) 1003–1034.